



**HAL**  
open science

## Structural control of collapse events inferred by self-potential mapping on the Piton de la Fournaise volcano (La Réunion Island)

Stéphanie Barde-Cabusson, Anthony Finizola, Aline Peltier, Marie Chaput, N. Taquet, S. Dumont, Zacharie Duputel, A. Guy, Lucie Mathieu, S. Saumet, et al.

### ► To cite this version:

Stéphanie Barde-Cabusson, Anthony Finizola, Aline Peltier, Marie Chaput, N. Taquet, et al.. Structural control of collapse events inferred by self-potential mapping on the Piton de la Fournaise volcano (La Réunion Island). *Journal of Volcanology and Geothermal Research*, 2012, 209-210, pp.9-18. 10.1016/j.jvolgeores.2011.09.014 . hal-01525729

**HAL Id: hal-01525729**

<https://hal.univ-reunion.fr/hal-01525729v1>

Submitted on 22 May 2017

**HAL** is a multi-disciplinary open access archive for the deposit and dissemination of scientific research documents, whether they are published or not. The documents may come from teaching and research institutions in France or abroad, or from public or private research centers.

L'archive ouverte pluridisciplinaire **HAL**, est destinée au dépôt et à la diffusion de documents scientifiques de niveau recherche, publiés ou non, émanant des établissements d'enseignement et de recherche français ou étrangers, des laboratoires publics ou privés.

# Structural control of collapse events inferred by self-potential mapping on the Piton de la Fournaise volcano (La Réunion Island)

S. Barde-Cabusson <sup>a,b,\*</sup>, A. Finizola <sup>c</sup>, A. Peltier <sup>d</sup>, M. Chaput <sup>a,c</sup>, N. Taquet <sup>a,c</sup>, S. Dumont <sup>a,e</sup>, Z. Duputel <sup>e</sup>, A. Guy <sup>e</sup>, L. Mathieu <sup>a</sup>, S. Saumet <sup>a</sup>, F. Sorbadère <sup>a</sup>, M. Vieille <sup>e</sup>

<sup>a</sup> Laboratoire Magmas et Volcans, Univ. Blaise Pascal-CNRS-OPGC, 5 rue Kessler, 63038 Clermont-Ferrand, France

<sup>b</sup> Instituto de Ciencias de la Tierra Jaume Almera (CSIC Barcelona), Barcelona, Spain

<sup>c</sup> Laboratoire GéoSciences Réunion, Université de la Réunion, Institut de Physique du Globe de Paris, Sorbonne Paris-Cité, UMR CNRS 7154, 15 avenue René Cassin, BP 97715 Saint-Denis cedex 9, La Réunion, France

<sup>d</sup> Institut de Physique du Globe de Paris et Université Paris Diderot, Sorbonne Paris-Cité, UMR CNRS 7154 – Géologie des Systèmes Volcaniques, 1 rue Jussieu, 75238 Paris cedex 05, France.

<sup>e</sup> Ecole et Observatoire des Sciences de la Terre, Université Louis Pasteur, Strasbourg, France

## ABSTRACT

Field surveys were performed on the terminal cone of Piton de la Fournaise in 2006 and 2008 to precisely map the self potential (SP) signal and determine the zonation of the hydrothermal activity both on the flanks of the cone and in the summit area, including inside the Bory and Dolomieu craters. SP maps inside the craters have been performed 8 months before the 5–7 April 2007 caldera collapse. Zonations appear both at the scale of the cone and of the summit and allow new interpretation of the electrical signal distribution on the terminal cone of Piton de la Fournaise. Superimposed to the SP maxima linked to the rift-zones, several areas of SP maxima associated with collapse structures have been detected: (1) in the summit area, the Bory and Dolomieu craters show the strongest SP values with amplitudes exceeding 2 V with respect to the base of the cone, and with a sharp lateral variation to the East, corresponding to the inner boundary of the Dolomieu caldera, collapsed on 5–7 April 2007, and (2) in the paleo pit craters surrounding the summit which show amplitudes similar to the Dolomieu–Bory craters. The analysis of the variations of the signal with time evidences a modification of the fluid flow pattern with a higher associated SP signature to the east in 2008. We interpret the amplification of fluid flow to the east in 2008 as a consequence of the eastward motion of the eastern flank of the volcano during the April 2007 eruption. The acquisition of SP data during two periods separated by the April 2007 eruption turns out to be a good opportunity to correlate the SP signal to the Piton de la Fournaise structure and to its evolution in term of hydrothermal and eruptive activity.

## 1. Introduction

The Piton de la Fournaise volcano is located on La Réunion Island, in the Indian Ocean. It is one of the most active volcanoes in the world with a mean of 2 eruptions per year since 1998 (Peltier et al., 2009a). The central active cone is located inside a U-shape depression formed by the Enclos Fouqué/Grandes Pentes/Grand Brûlé, a major structure opened on the Indian Ocean (Fig. 1). The origin of this structure (collapse, sliding or combination of both processes) is still debated. In the past 4.5 ka, the eruptive activity usually took place inside this U-shape depression and only a few eruptions occurred beyond its limits (Bachèlery, 1981).

The summit of the terminal cone is characterized by the presence of two collapse craters: Bory and Dolomieu (Fig. 1). In the past 200 years, the Bory crater did not experience major volcanic or tectonic activity of

its own (Lénat and Bachèlery, 1990). On the other hand, the Dolomieu crater morphology was ceaselessly reshaped by successive collapse and eruptive events. The Dolomieu crater was the result of the coalescence of several pit craters and, until April 2007, the crater floor was leveled by accumulated lava flows and projections emitted by summit eruptions (Lénat and Bachèlery, 1990). During the large April 2007 eruption, the Dolomieu crater was affected by a major collapse increasing its depth to 340 m (Michon et al., 2007a; Urai et al., 2007). Today, the eruptive activity is slowly refilling the crater.

On the Piton de la Fournaise volcano, multiple SP studies have already been carried out in the Enclos Fouqué structure, on the terminal cone (Lénat, 1987; Malengreau et al., 1994; Zlotnicki et al., 1994; Michel and Zlotnicki, 1998) and/or on outlying areas of the massif (Boubekraoui and Aubert, 1999; Levieux, 2004; Lénat, 2007; Barde-Cabusson et al., 2009). Malengreau et al. (1994) and Michel and Zlotnicki (1998) produced self-potential maps of the terminal cone and the surrounding areas (some are presented in Fig. 2). They evidenced the coincidence of high SP values (with respect to the surrounding areas) with the three main eruptive axes of the volcano, i.e. the northern and southern rift

\* Corresponding author at: Instituto de Ciencias de la Tierra Jaume Almera (CSIC Barcelona), Barcelona, Spain. Tel.: +34 934095410.

E-mail address: s.barde.cabusson@gmail.com (S. Barde-Cabusson).

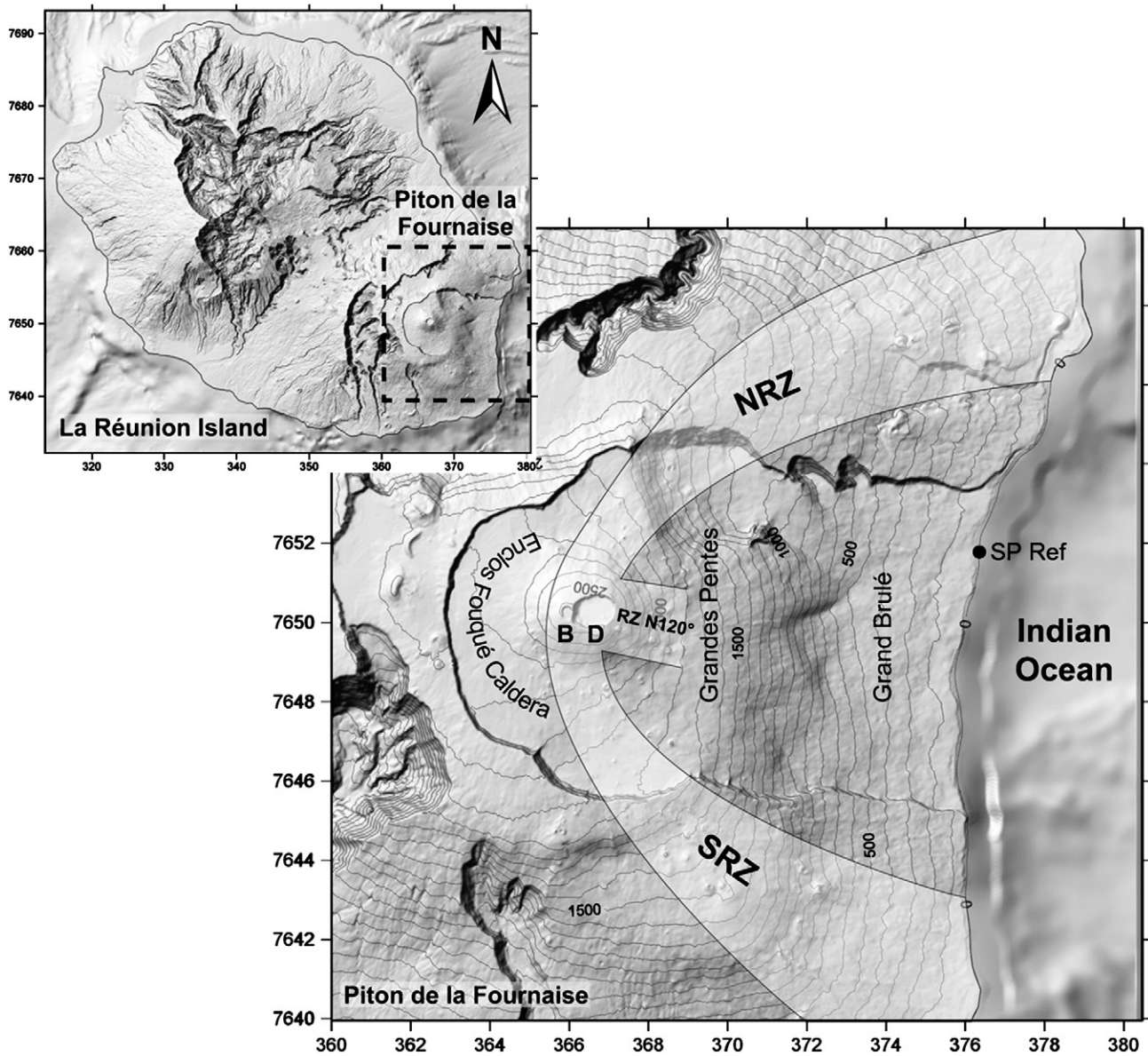


Fig. 1. Overview of the main features of La Réunion Island discussed in the text. B: Bory crater; D: Dolomieu crater; NRZ and SRZ: northern and southern Rift Zones.

zones and the N120° rift zone, also well-known as a major structural orientation for the island (Bachèlery, 1981; Michon et al., 2009a; Fig. 1).

At a lower scale, Malengreau et al. (1994) attributed the SP maxima recorded in the summit area to the hydrothermal activity around the magma reservoir. Lénat et al. (2000) supported this hypothesis from the interpretation of direct current electrical and transient electromagnetic soundings. The authors interpreted the low resistivity zones inside the cone as altered rocks of the hydrothermal system. In their interpretation, hydrothermal fluid circulation is thus implicated to explain both the SP positive peak and the low resistivity zone.

Even if these previous SP studies identified the main eruptive axes draining hydrothermal fluids, data spacing and measurement distribution did not allow discriminating in detail the smallest structures, especially at the summit, an area strongly affected by fractures. However it is important regarding the recent evolution of the summit area to well constrain the active structure controlling its eruptive activity and its collapses. So, we carried out new detailed SP measurements in order to constrain more precisely the structural limits and the active hydrothermal zones at different scales from the edifice (terminal cone) to the summit, taking into account the previous hydrological models on Piton de la Fournaise (Join et al., 2005).

This paper presents the results of a self-potential study employed in characterize the electric signal on the Piton de la Fournaise terminal cone. The data is discussed to determine the distribution of the hydrothermal activity and its relations with the structure and dynamics of this volcano. We also discuss the data in relation with the April 2007 Dolomieu collapse.

## 2. Data acquisition and processing

Self-potential (SP) signals refer to quasi-static electrical potential anomalies, usually measured at the ground surface of the Earth, that are associated with the occurrence of source current densities existing at depth (Sill, 1983; Corwin, 1997). Various sources can generate a difference of potential, but on active volcanoes, the main source of SP anomalies is related to the flow of the groundwater (Massenet and Pham, 1985; Ishido et al., 1997; Bedrosian et al., 2007). In this case, self-potential signals is generated by the streaming potential effect, related to the flow of the pore water relative to the mineral grain framework in saturated (Overbeek, 1952; Nourbehecht, 1963) and unsaturated conditions (Revil and Cerepi, 2004; Linde et al., 2007). The fact that the SP signal is generally positive in the flow direction



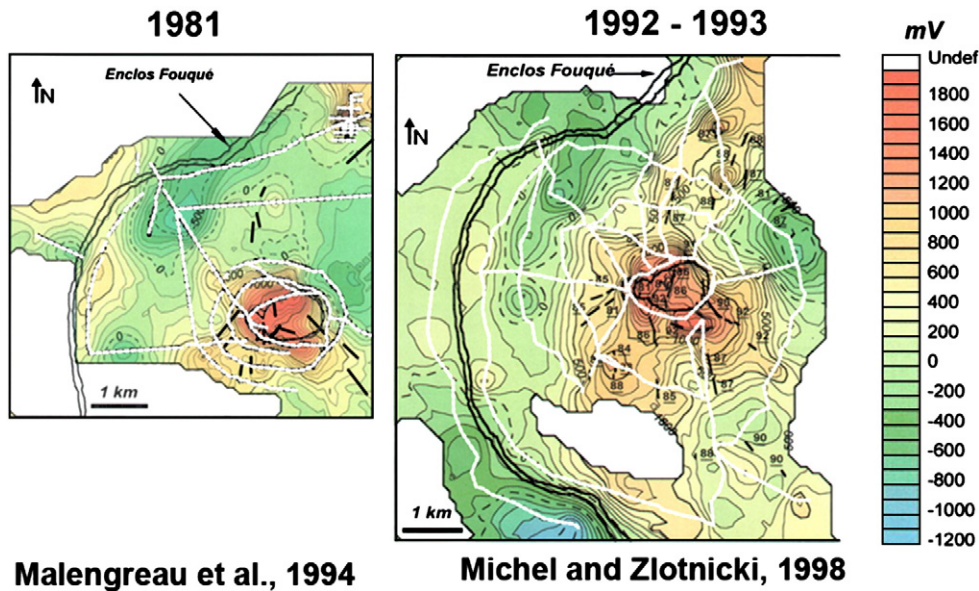


Fig. 2. Self potential maps obtained in 1981 and 1992–93. White dotted lines correspond to the location of the measured points (variable spacing).

can be understood thanks to the electric double (or triple) layer theory describing the electrochemical interactions occurring at the interface between a mineral and the pore water (e.g. Revil, 2002 and references therein). In active volcanoes, pH of the hydrothermal system can range from low ( $\sim 2$ ) to high ( $> 10$ ) values. However, experimental results (Revil, 2002) generally gives pH in the range 5–8, and therefore the zeta potential is usually negative. The surface of silicate and aluminosilicates of volcanic rocks is negatively charged. The corresponding negative fixed surface charge is counterbalanced by a mobile charge in the so-called electrical diffuse layer. The diffuse layer has a net charge of opposite sign to the surface charge of the mineral to maintain a global electroneutrality in the system. The flow of pore water drags most of the mobile positive charges of the electrical diffuse layer in the flow direction, generating a positive electric self-potential at the ground surface. Most hydrothermal systems associated with active volcanoes evidence a large positive SP anomaly in the area where fluid flow is upwelling (e.g. Revil, 2002; Ishido, 2004; L  nat, 2007). However, it is important to note that in some cases rocks are positively charged in neutral pH conditions and that some volcanoes showing geothermal activity on their flanks have shown no positive anomalies associated (Guichet and Zuddas, 2003; Hase et al., 2003; Aizawa, 2008; Aizawa et al., 2008). Therefore, in absence of laboratory experiments to measure the zeta potential of the rocks, the classic interpretation of SP data (hydrothermal upwelling corresponding to positive SP zone) constitutes only an assumption.

We acquired a dense dataset of 4621 self-potential measurements (SP) on the Piton de la Fournaise volcano in July and August 2006, i.e. 8 months before the large April 2007 eruption and Dolomieu collapse. We repeated the summit SP mapping in May 2008, one year after the Dolomieu collapse. The SP equipment consisted of a high-impedance voltmeter ( $\sim 10$  M $\Omega$ ), a pair of Cu/CuSO<sub>4</sub> non-polarizing electrodes and an insulated copper cable. During the measurements, the reference and moving electrodes were switched every few hundred meters in order to avoid the systematic error due to electrodes offset. We controlled the contact between the electrodes through the ground by checking the electric resistance before each measure point. As a rule of thumb, the electrical resistance between the two electrodes should be always ten times smaller than the internal impedance of the voltmeter (Corwin, 1997).

Data were acquired along 12 profiles crossing the entire terminal cone, a circular loop around the base of the cone, and a loop around the summit craters with a regular spacing of 20 m (Fig. 3b). In addition, we performed a denser measurement network in the summit area with 24

radial lines outside the craters with a 2 m spacing, 15 radial lines from the center of the Dolomieu crater, 4 from the center of the Bory crater, and 2 circular profiles along the craters inner walls with a 20 m spacing (Fig. 3a, c, and d). The whole measurement network is interconnected so that we applied a closure correction along the loops, in order to limit cumulative errors. The order of magnitude of the closure correction is of a few tens of millivolts. Usually the 0 mV reference for SP measurements is taken at the sea or a water table as it provides a constant value in time. Given no such stable reference is available in the studied area, we used the self-potential map of a former study to connect our dataset to the sea (data from Leveux, 2004 and L  nat, 2007). The datasets were joined in at point X 364.709, Y 7650.933 (UTM-WGS84, km), in a zone where the hydrothermal and eruptive activity is scarce (black arrow on Fig. 3b).

### 3. Data analysis

In this section, we first describe the results obtained from the wide-scale SP map of the terminal cone of Piton de La Fournaise and, in a second time, we detail the repartition of the anomalies in the summit area.

#### 3.1. Self-potential map of the terminal cone

The entire cone is characterized by negative self-potential values relative to the sea. On a typical profile crossing an active volcanic cone, the SP variations are axis-symmetrical and a radial cross-section generally displays a W-shape centered on the cone (e.g. Ishido et al., 1997; Zlotnicki et al., 1998; Revil et al., 2003; Finizola et al., 2004; Ishido, 2004; L  nat, 2007). On the Piton de la Fournaise, the SP map of the terminal cone, which we will consider as a reference pattern, shows a continuous increase of the SP values from the base of the cone to the summit area (Fig. 3b). We found an average SP/elevation gradient of 1.3 mV/m (ranging from 0.2 to 3.7 mV/m) along profiles on the flanks of the terminal cone; the average gradient along the 24 radial profiles around the crater is of 7 mV/m (ranging from 3.1 to 15 mV/m and with profile 6 showing a gradient of  $-12.2$  mV/m); for the Dolomieu and Bory craters, the SP/elevation graph shows a quasi-vertical alignment of the points (Fig. 4). The highest SP variation from the base of the cone to the craters is about 2.3 V. The northern, southern, and eastern flanks are the seats of three main elongated radial anomalies compared to the reference pattern (Fig. 3b).

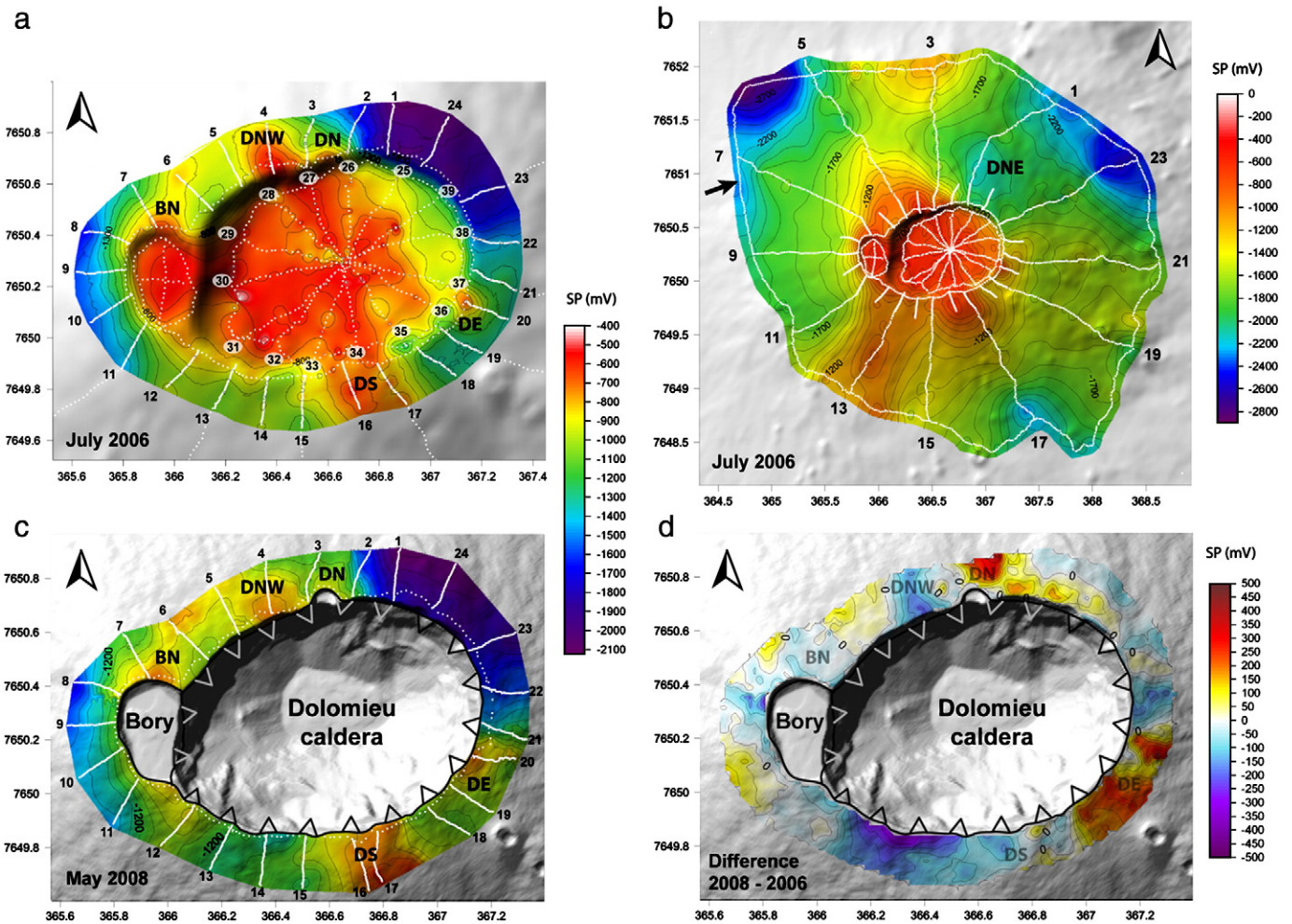


**Fig. 3.** (a) Self potential maps of the summit area of the Piton de la Fournaise in 2006, and (c) 2008, (d) difference between them, and (b) self potential map of the terminal cone in 2006. BN stands for Bory north, DNW for Dolomieu north-west, DN for Dolomieu north, DNE for Dolomieu north-east, DE for Dolomieu east, and DS for Dolomieu south. White dots are the measured points, black numbers refer to the profiles, and the black arrow points at the measured point used to connect our dataset to a previous one (Levieux, 2004 and Lénat, 2007) in order to reference our maps to the sea (see text). (For interpretation of the references to color in this figure legend, the reader is referred to the web of this article.)

A radial SP anomaly extends on the northern flank with a roughly N150° direction, near the crater, shifting to a N10° direction in the lower part of the cone (Fig. 3b). The southern flank is affected by a N25°

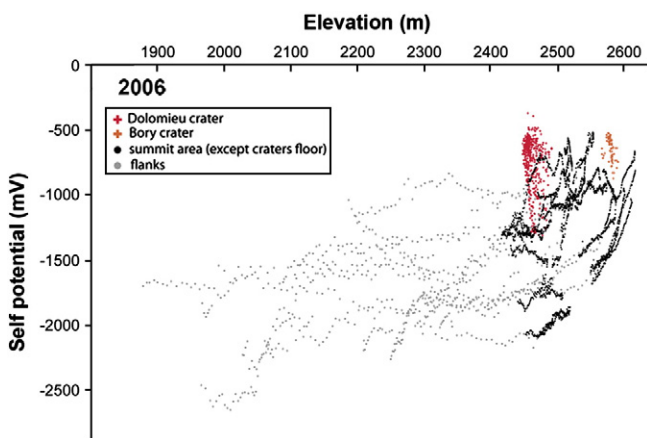


**Fig. 4.** Plot of elevation versus SP for the 2006 dataset of Piton de la Fournaise. Note the globally positive correlation between SP and elevation over the whole dataset. The global gradient was estimated graphically, plotting the corresponding trendlines for the flanks of the cone and for the summit area (profiles surrounding the craters) data. The value for each profile has also been estimated to give a range of the values encountered (see text).

similar radial anomaly. Each of these two elongated anomalies is about 1 km large and defines a SP maximum of about 1 V amplitude with respect to the surrounding areas. Farther east and west from those main axes the SP anomalies vanish progressively. They seem to extend on both sides of the summit area, in the north and in the south, beyond the investigated area.

On the eastern flank of the cone, a more diffuse SP maximum, outlined by the SP contour lines, highlights a significant anomalous zone (profiles 19 and 21 on Fig. 3b). The maximum SP value is about -1600 mV in the lower part of the cone (at an elevation of 1900 m), and higher in the crater vicinity. It means the anomaly is about 400 mV and 600 mV lower than the maximum values registered on the northern and southern flanks respectively.

Fig. 5 shows a good correlation between the location of the eruptive fissures since 1981 and the position of the SP maxima. In particular the most recent eruptive fissures are located on the highest SP values and their repartition follows a very similar orientation than that of the northern and southern rift zones. In the NNE direction, no SP maximum anomaly appears, while eruptive fissures exist. However this direction is barely followed by dykes, compared to the rift zones. Only 4 dykes affected this direction in 35 years (Peltier et al., 2009a).

These three main elongated anomalies were already visible in 1992–1993 and also in 1981 but with a lower amplitude on the northern one (Fig. 2; Malengreau et al., 1994; Michel and Zlotnicki, 1998).



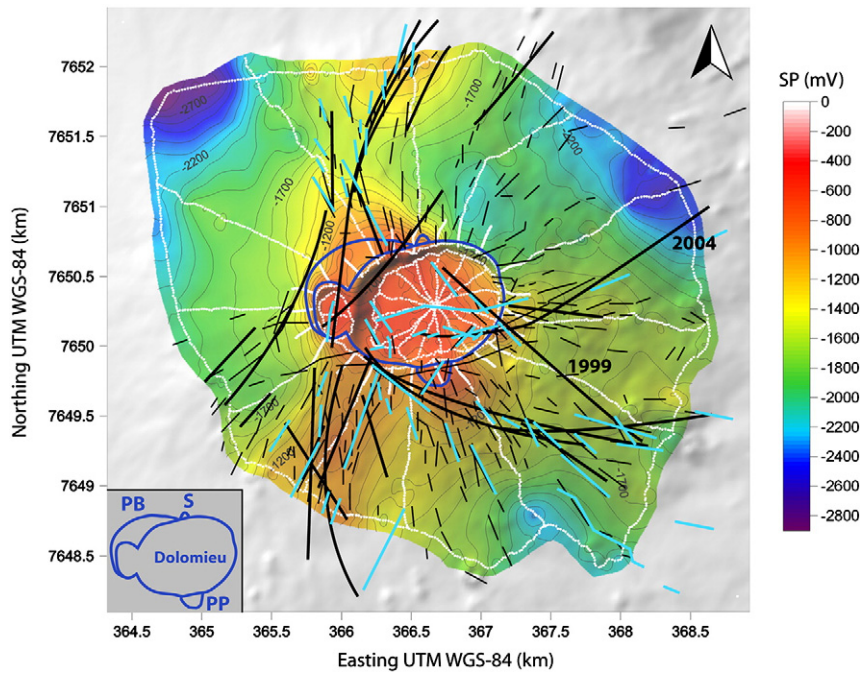


**Fig. 5.** Distribution of the eruptive fissures visible in the field (thin black line, after Michon et al., 2009a). Light blue lines are eruptive fissures from 1998 to 2007 (Peltier et al., 2009a). The bold black lines are the estimated dyke location associated to proximal eruptions between 1981 and 2006 from Michon et al. (2009a). PB stands for Pre-Bory pit crater, S for Soufrière pit crater, and PP for Petit Plateau pit crater. Dark blue lines are the major structural limits influencing SP measurements (see text). (For interpretation of the references to color in this figure legend, the reader is referred to the web of this article.)

### 3.2. Detailed self-potential map of the summit area

#### 3.2.1. Self-potential zonation along the crater boundaries

With a color scale adapted to the SP amplitude of the summit area, interesting information appears about the SP signal zonation (Fig. 3a and c). The strongest anomalies are centered on the Bory and Dolomieu craters. A significant SP difference of up to several hundred millivolts exists between the crater floor and the rims of these two craters, except (1) on the northern border, close to profiles 3–4, (2) on the northwestern border, on profile 7, and (3) on the southeastern border, between profiles 15 and 21. For instance, in the northeastern side of Dolomieu, we observe a difference of approximately 600 mV between the rim and the Dolomieu crater floor. The usual hydrogeological gradients observed on the inactive flanks of Piton de la Fournaise (i.e. topographic effect) ranges between 0 and  $-3$  mV/m (Lénat, 2007). The northeastern crater wall was about 30 m high at the time of the survey, which is too small to explain such a difference of electrical potential by a topographic effect. Moreover, it is interesting to note that along the north–south rift zone axis, five profiles also displays strong SP variations (of several hundreds of mV) between the rim and the floor of Dolomieu crater (see profiles 5, 6, 12, 13 and 14 on Fig. 3a).

#### 3.2.2. Self-potential zonation inside the Dolomieu crater

On Fig. 3a the amplitude of the SP signal and the orientation of the isolines highlight a clear zonation between the eastern third and the rest of the Dolomieu crater (also see Fig. 6). The eastern part of the Dolomieu crater is marked by a nearly E–W SP spatial variation from  $-1100$  mV along the crater wall up to  $-500$  mV near the center of the crater, 500 m farther. The isolines show a NNW–SSE orientation while they do not follow a particular direction on the rest of the crater floor. This feature observed on a flat area reflects a clear heterogeneity of the Dolomieu crater structure before the April 2007 collapse.

#### 3.2.3. Self-potential anomalies around the craters

On the external edge of the Dolomieu and Bory craters, five small-scale SP maxima are individualized (red-orange color in Fig. 3a and c). These anomalies are located respectively: (1) south of the Dolomieu

crater, crossing profiles 16 and 17 (DS in Fig. 3a and c), (2) north of the Dolomieu crater, crossing profile 4 (DNW in Fig. 3a and c), (3) north of the Bory crater, crossing profile 7 (BN in Fig. 3a and c), (4) north of the Dolomieu crater between profiles 2 and 3 (DN in Fig. 3a and c), (5) south-east of the Dolomieu crater, crossing profile 20 (DE in Fig. 3a and c).

- (1) In the south, the DS anomaly is 200–250 m wide and globally superposed to the Petit Plateau paleo-pit crater. This later formed around 1791 (Bachèlery, 1981), consists in surface of a system of concentric fractures that delineates the hidden collapsed structure (Peltier et al., personal communication). This is one of the areas showing the maximum fracture and fissure density around the Dolomieu crater (see Fig. 5 and Michon et al., 2009a). The related SP maximum has a wider extension than the superficial structural boundary of the Petit plateau pit crater (Fig. 5).
- (2) The DNW SP anomaly to the north of Dolomieu (profile 4 on Fig. 3a and c) corresponds as well to a highly fractured zone. It is related to the hidden boundary of a larger paleo-pit crater named Pre-Bory pit crater (see Fig. 5; Lénat and Bachèlery, 1990; Michon et al., 2009a). Large part of this SP maximum is located just inside the boundary of Pre-Bory pit crater.
- (3) The BN SP anomaly (profile 7 on Fig. 3a and c) is located also just inside the Pre-Bory pit crater limits and seems to extend at least up to the northern extremity of profile 6 with a slightly lower SP amplitude.
- (4) The DN SP anomaly (between profiles 2 and 3 on Fig. 3a and c) is located close to the Pre-Bory pit crater but corresponds to another structural boundary named Soufrière pit crater, formed in 1964 (Fig. 5; Carter et al., 2007).
- (5) The DE SP anomaly (profile 20 on Fig. 3a and c) located on the eastern border of Dolomieu, did not appear on the 1981 SP map (Malengreau et al., 1994) but was present in 1992 (Fig. 2: map from Michel and Zlotnicki, 1998) and still exists in 2006 (our survey). Strikingly, several dykes (18–19 December 1975, September 1985, January 1990, July 1991, July 1999 and August 2004 dykes) cross this particular point. Shortly after our survey, the 30 August 2006 eruptive fissure crossed

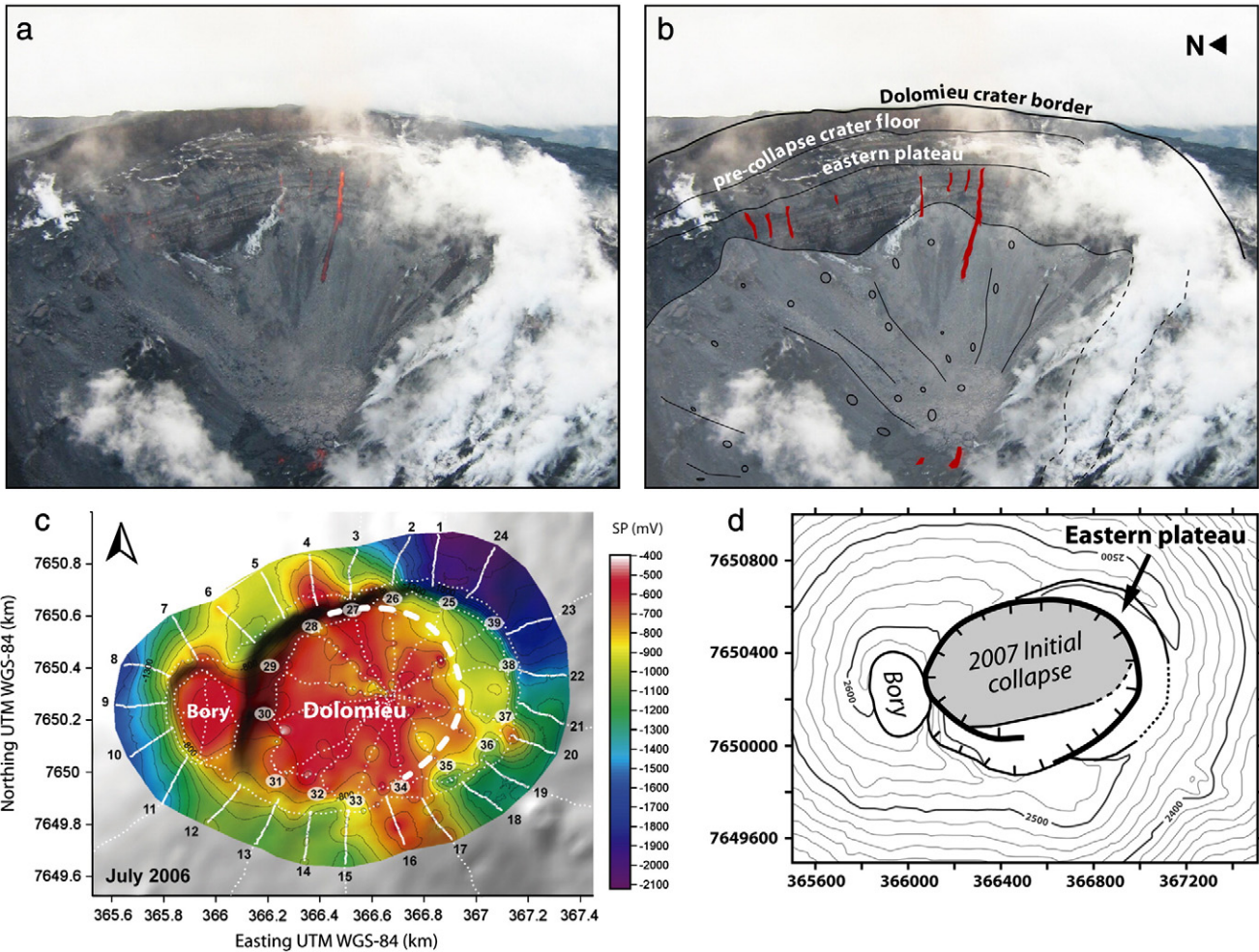


**Fig. 6.** (a) Photo taken on the 6th April 2007 (courtesy of “Gendarmerie nationale”) from Bory crater, looking at the east and (b) its interpretation; red shapes correspond to fresh lava flows emitted during the 30 August 2006–1 January 2007 eruption, and not yet cold in subsurface in April 2007. (c) On the eastern side of the Dolomieu crater, our 2006 SP map shows a pattern that can be interpreted as the control of the hydrothermal circulation by a pre-existing fault inside Dolomieu (white strokes). In 2007 this structure led to the formation of the eastern plateau during one stage of the Dolomieu caldera collapse. (d) Schematic structural map from Michon et al. (2007a). (For interpretation of the references to color in this figure legend, the reader is referred to the web of this article.)

the crater wall at the same point as the December 2003 eruption did before.

Even if the position of the main anomalies is not modified from one survey to the other, by calculating the difference between the 2008 and 2006 SP maps (Fig. 3d) we can evidence a significant variation of the amplitude of the signal in several areas. We identify an increase of the SP signal at the eastern limit of the northern and southern rift zones and in the southern part of the N120° rift zone, around the Dolomieu crater, (red shades) and a decrease of the signal on the southern rift zone and in part of the northern rift zone (dark blue shades).

#### 4. Discussion: self potential as a marker of the structures controlling eruptive and collapse events

The entire cone is characterized by negative self-potential values relative to the sea. The SP distribution depends on the hydrogeological pattern of the study area. Recent studies show that cold and dilute descending groundwater is important for SP generation (Ishido, 2004; Aizawa et al., 2009). Basically, they show that negative SP zones generated by infiltration are the actual anomalies while the SP maxima are created by the surrounding minima. In the case of Piton de la Fournaise, Join et al. (2005) simulation gives hydraulic confirmation of a the

presence of a continuous aquifer and of a central groundwater dome. In the Enclos Fouqué Caldera (Fig. 1), the water table is then nearly parallel to the topography (Join et al., 2005). Taking a reference at the sea means we consider the water table is at sea elevation and that the interpretation of SP negative anomalies is downward fluid flow (e.g. see Lénat, 2007). Following the hydrogeological model proposed by Join et al. (2005), in our maps, hydrothermal upwelling will then be marked by SP maxima and positive SP/elevation correlations and infiltration by some SP minima and negative SP/elevation correlations. Moreover, we will interpret the SP data jointly with information from Lénat et al. (2000) on the resistivity structure of the terminal cone and their interpretations in term of hydrothermal activity.

In the typical W-shaped SP signal of active volcanic cones cited before, some authors interpret the two minimums of the W signal as the transition between the hydrogeologic SP signature of the lower flanks (negative SP/elevation correlation) and the hydrothermal SP signature of the upper part of the edifice (positive SP/elevation correlation) (e.g. Zlotnicki et al., 1998; Finizola et al., 2004; Lénat, 2007). Just considering the terminal cone of Piton de la Fournaise volcano, no W-shape signal and very few negative SP/elevation correlations have been observed (Fig. 4). At the scale of the Enclos Fouqué caldera, in the western part, along the SP maximum evidenced by Michel and Zlotnicki (1998) is possibly compatible with a transition to the hydrogeological area but the relationship between



SP signal and elevation cannot be established (flat topography in this area). The amplitude of the SP signal on the three main positive SP radial anomalous areas and the positive SP/elevation correlation encountered on all the flanks of the terminal cone, strongly suggests (1) that the whole terminal cone of Piton de la Fournaise is affected by rising of hydrothermal fluids and (2) that the summit craters and the northern, southern, and eastern axes are preferential paths for hydrothermal fluids.

The strong hydrothermal rising fluids preferentially located in the upper part of the cone and along the three rift zones can hide the presence of infiltration in the surrounding areas. An exception is found along profile 1 (Fig. 3b) that shows a SP minimum (DNE) associated to a negative SP/elevation gradient ( $-1.25$  mV/m). This suggests that DNE minimum could evidence a preferential downward water flow pathway (Fig. 7).

The detailed summit SP map and the general SP map of the entire cone of the Piton de la Fournaise volcano offer a good opportunity to discuss the importance of the structural boundaries in controlling hydrothermal fluid flows and potentially magmatic injection. The general SP map shows that the entire edifice is affected by hydrothermal activity, but with different intensities from an area to another.

Ishido (2004) demonstrated that, if an electrical conductive structure (as hydrothermally altered rock) extending to deep levels is present below the summit area of a volcanic cone, SP around the summit is substantially increased, resulting in the characteristic strong positive anomaly observed in this area of active volcanoes. Considering the ambiguity in interpreting SP data alone (Finizola et al., 2006; Revil et al., 2008; Finizola et al., 2009), it is interesting to compare our SP results and interpretation (see Fig. 7) with the electrical resistivity measurements obtained by Lénat et al. (2000), on the same area, in 1987–1992. The authors led a study of the geoelectrical structure of the central part of Piton de la Fournaise volcano. Beneath the highly active summit area, the authors observed an electrical conductor rising below the terminal cone (resistivity values  $<20 \Omega\text{m}$  below  $\sim 500$  m depth and  $<250 \Omega\text{m}$  from  $\sim 500$  m up to  $\sim 300$  m depth) that they interpreted as an altered hydrothermal zone. The overburden is composed of resistive terrains ( $1000$  to  $3000 \Omega\text{m}$  and  $>8000 \Omega\text{m}$  for the shallowest  $100$  m), typically interpreted as water-sparse region, not significantly affected by hydrothermal circulation (e.g. Aizawa et al., 2009; Garcia and Jones, 2010; Revil et al., 2010). On Piton de la Fournaise, fresh lava flows show resistivity ranging  $10,000$  to  $100,000 \Omega\text{m}$  so that resistivities of  $1000$  to

$3000 \Omega\text{m}$  can mean a weak hydrothermal circulation. However, areas affected by intensive hydrothermal activity are usually characterized by resistivities ranging from a few  $\Omega\text{m}$  to few hundreds  $\Omega\text{m}$  (e.g. Revil et al., 2004, 2008; Finizola et al., 2009, 2010; Revil et al., 2011). In our survey performed in July 2006, 9 months before the April 2007 caldera collapse, several evidences attest to an intensification of the hydrothermal activity in the shallower part of the cone below the craters, with respect to the conditions during the 1987–1992 period (Lénat et al., 2000): (1) The sharp SP horizontal gradient ( $\sim 1000$  mV in a few tens of meters) between the inner and external parts of the Dolomieu crater (Fig. 3a) suggests a shallow and strong lateral variation in the fluid circulation pattern and/or in the resistivity structure. (2) Just after the April 2007 collapse, hot areas have been observed on the ground surface through IR camera inside the Dolomieu collapse structure (Staudacher, 2010), and (3) hydrothermal alteration has been observed along the cliffs left by the 2007 Dolomieu caldera collapse between the surface and  $300$  m depth (Peltier et al., personal communication). Because resistivity is highly sensitive to hot and mineralized volcanic fluids like hydrothermal fluids, it is possible that the resistivity structure changed between 1987–1992 and 2006 due to the hydrothermal/magmatic activities (Aizawa et al., 2011, and reference therein). The top  $300$  m beneath Dolomieu crater may have turned to be affected by more intense hydrothermal activity before the 2007 collapse, responsible for the strong SP maxima measured in July 2006 in the crater area. Based upon these considerations we can interpret the signal observed on Piton de la Fournaise in terms of spatial variations of underground hydrothermal activity.

If some geological and geophysical clues have been found to constrain the shallowest part of the hydrothermal system before the 2007 collapse event, it is not easy to infer the hydrothermal circulation condition at depth from SP data alone. SP sources being broadly distributed in the volcanoes (Yasukawa et al., 2005; Aizawa et al., 2009), the large wavelength ( $\sim 1$  km) superimposed on the northern and southern rift zones (Fig. 5) do not give a strong constrain on the depth of the SP source. Considering the results obtained by Lénat et al. (2000), with resistivity values  $<20 \Omega\text{m}$ , up to the maximum depth of investigation ( $\sim 1000$  m below the surface), we can reasonably assume that the hydrothermal system is intensively active up to that depth. Below  $1000$  m depth, we have no data to constrain the hydrothermal fluid flow, as shown in Fig. 7.

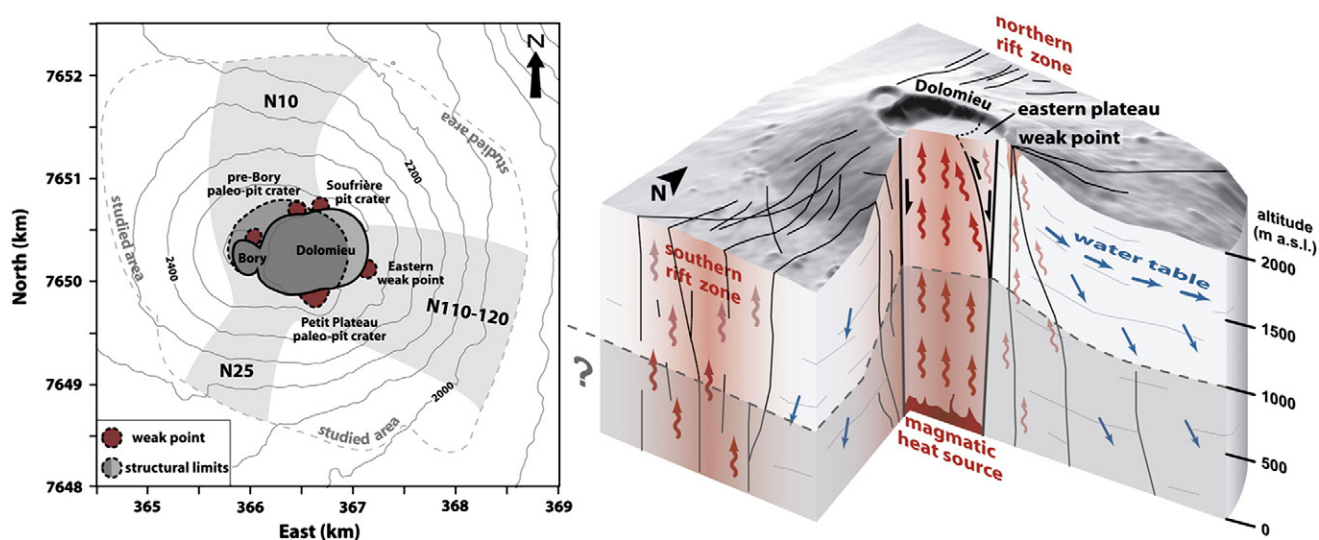


Fig. 7. Synthetic map (left) and 3-D block (right) of the main features evidenced by the self potential signal and of our main conclusions. In the synthetic map, N10°, N25°, and N110–120° refer to the direction of the rift zones (light-grey areas). The red points refer to the five SP maximum evidenced around Dolomieu and Bory craters. In the 3-D block, the black arrows highlight the main structural limits involved in the Dolomieu April 2007 collapse; the red arrows represent rising hydrothermal fluids. Hydrothermal circulation at depth is constrained up to  $1000$  m below the topography using electrical resistivity data from Lénat et al. (2000). The blue arrows represent infiltration and lateral cold groundwater flow (water table) as proposed by Join et al. (2005). (For interpretation of the references to color in this figure legend, the reader is referred to the web of this article.)



Based on our SP study, we highlight the main zones of hydrothermal release of the Piton de la Fournaise and describe various types of structural boundaries:

- (1) *Summit crater boundaries*: The major structure draining hydrothermal fluids is the Dolomieu–Bory crater zone (Fig. 3). The Dolomieu–Bory boundary is a well-known structural limit. Major part of the dykes associated to summit and proximal eruptions start around this limit (Peltier et al., 2009a). The main SP anomaly then underlines the major role of this area on the magma transit to the surface on Piton de la Fournaise. The border faults of these two craters (Fig. 5) constitute a major structural barrier reducing drastically the radial diffusion of hydrothermal fluids into the ground, outside the craters. The importance of the Dolomieu–Bory structural boundaries on the control of hydrothermal fluid flow between the inner and the outer part of the Dolomieu–Bory craters is also attested by the data collected after the 5–7th April 2007 Dolomieu caldera collapse. Indeed, the location of the main anomalies on the SP maps of the summit area realized before (July 2006) and after (May 2008) the Dolomieu collapse is similar (Fig. 3a and c). This means that this major collapse event did not affect significantly the fluid flow pattern in the vicinity of the collapsed area. This can be easily understood through the geological evolution of the summit area, which has been affected by several collapse and pit-crater events. The most recent ones inside the Dolomieu crater took place between 1931 and 1935 (east), in 1953 (southwest), in 1961 (southwest), in 1986 southeast), in 2002 (southwest) and in 2007 (the whole Dolomieu crater) (Peltier et al., 2009b). These events were alternated with periods of eruptive activity refilling the craters through the accumulation of lava flow. The succession of collapse events along the same crater limits (the current Dolomieu–Bory limits) demonstrates the individualization of a rock column delimited by the Dolomieu–Bory boundaries. Such individualization of a rock column explains the localization of the main hydrothermal fluid circulations inside the craters and why the last collapse of April 2007 does not affect significantly the hydrothermal fluid flow pattern. Also, the absence of significant changes in the position of the SP anomalies and the absence of amplitude variation for most part of this area between July 2006 and May 2008 (Fig. 3a, c, and d) after such a collapse, attest that the pre-existing Dolomieu–Bory structural boundaries were acting as a barrier for lateral fluid flow before the April 2007 collapse. Inside the Dolomieu crater, another structural barrier for fluid flow has been evidenced in the eastern side of the crater. The SP zonation previously described affects the whole Dolomieu crater with a NNW–SSE orientation of the SP isolines on the eastern side of the crater. There was no significant zonation related to the repartition of the recent lava flows and eruptive vents or fissures on the Dolomieu floor. These considerations make highly improbable the hypothesis of shallow hydrothermal SP sources influencing the observed SP pattern. Rather than a shallow transient anomaly, we think that the SP signal in Dolomieu was revealing a hidden pre-existing fracture or fault system to the east controlling the hydrothermal fluid rising from depth in the crater (Figs. 6 and 7). This hypothesis matches the interpretation proposed by Michon et al. (2009b) on the Dolomieu caldera collapse process. The authors show that the structure of the new Dolomieu caldera and its evolution during the collapse is explained by the collapse of a coherent block limited by vertical to outward dipping fractures at depth and sub-surface normal fractures. According to the first observations, on April 7, 2007, the Dolomieu collapse affected first the western and the northern part of the pre-existing Dolomieu crater while a wide annular plateau corresponding to the pre-existing floor of Dolomieu was remaining in the east (Michon et al., 2007a). On April 10 the caldera was enlarged and

only few perched terraces remained from the eastern plateau. The authors add that the similar contours of Dolomieu before the collapse and of the new caldera, remarkably shows the control of the pre-existing structures in the April 2007 caldera collapse. In the same way, we think that the inner structure of the crater controlled the successive phases of the collapse and that the SP signal was marking this particular structure at least 1 year before the collapse. The Dolomieu collapse would result from the combined effect of a progressive destabilization of the rock column above the magma chamber since 2000, and the large amount of magma withdrawal during the early stage of the 2007 eruption (Michon et al., 2007a; Peltier et al., 2009b). The eastern plateau remaining in the first phases of the Dolomieu collapse may be associated to a pre-existing east-dipping fracture individualizing an eastern block in the rock column beneath Dolomieu. The fracture draining hydrothermal fluids, this block may have been relatively isolated from the rest of the crater in terms of fluid advection. This would explain a SP signal progressively decreasing from a hidden fracture to the inner part of the isolated block. Our data matches with a more or less N–S fracture running from the middle-eastern part of Dolomieu at shallow depth to the eastern edge of the crater at depth (Fig. 6).

- (2) *Pit crater boundaries*: Just outside the Dolomieu and Bory craters, we evidenced thanks to our high resolution map small scale positive anomalies whose amplitudes are similar to the highest amplitude inside the Dolomieu and Bory craters. The anomalies of highest amplitude are related with three old pit-crater structures, which are Petit Plateau, Pre-Bory, and Soufrière (see Figs. 5 and 7 for location). In all these cases, the former pit craters cut either the Dolomieu and/or the Bory crater rims. Considering that pit craters are highly fractured zones, they constitute more permeable areas explaining the local rise of hydrothermal fluid flow, of same intensity than inside the Dolomieu and Bory craters. On another hand, the SP anomaly related to the Petit Plateau pit crater being larger than the surface fracture network, a hidden and larger collapse structure could be associated to this structure, at depth (Fig. 5).
- (3) *Temporally dyke injection pathways*: The only small scale maximum SP anomaly not related with pit crater structure, and already visible in 1992 (Fig. 2) is the south-eastern Dolomieu anomaly (DE on Fig. 3a and c) located on the N120° rift zone and associated to dyke intrusions feeding eruptions close to this area. Three eruptions associated to eruptive fissures and dykes have been crossing recently this site (e.g.: in July 1999, August 2004, and August 2006; Figs. 5 and 7). It is possible that this area was draining hydrothermal fluids along a major structure of the edifice where dykes are preferentially injected. This SP anomaly was already visible on the map made by Michel and Zlotnicki (1998; Fig. 2) in 1992, a few months after the July 1991 eruption and two years after the January 1990 eruption, which occurred both in this area. On the map of 1981 (Malengreau et al., 1994; Fig. 2), no such anomaly is visible revealing that the SP intensity in this area is directly related to dyke emplacement; indeed in 1981 the last dyke injected in this area was in December 1975. So this anomaly can be due to (1) the opening and re-opening of fractures during dyke injections east of the Dolomieu crater which favor temporally deep fluid hydrothermal circulation in this area or to (2) the shallow advection of fluids in the first meters of the ground in recent emplaced lava flows (Barde-Cabusson et al., 2009).
- (4) *Main rift zone pathways*: Other maximum SP anomaly corresponds to the three main axes pointing to the summit area. The diffuse N110–120° axis corresponds also to a main direction of La Réunion Island associated with the lithospheric structural anisotropy located beneath the island (Michel and Zlotnicki, 1998; Michon et al., 2007b). We can distinguish the main N–S axis, corresponding to the well-known rift zones, and this secondary

N110–120° axis of lower intensity. These highly fractured zones are preferential pathways for hydrothermal rising fluids and are thus zones of major permeability and of low mechanical resistance and therefore of major probability of eruption. Indeed, these high permeability areas are preferential pathways for both fluid from the hydrothermal system or for magma rising from depth. On Piton de la Fournaise like in all active hydrothermal fields, the amplitude of the SP anomalies can vary with time (Fig. 2; e.g.; Michel and Zlotnicki, 1998) without changing their spatial distribution, revealing that they are strongly controlled by the structure of the edifice i.e. by the lithological contrasts, the repartition of the fractures and eruptive fissures. It is then not surprising that the preferential hydrothermal circulation underlines the well-known northern and southern rift zones of the volcano (Figs. 2, 3, and 5).

The rift zones concentrate recent vents, dykes, eruptive fissures and young lava flows (Fig. 5). Since 1998, the activity of Piton de la Fournaise has been characterized by an average of two eruptions per year producing mostly lava flows. As a consequence, the recent (<10 years) lava overburden is significant on the rift zones. Therefore, the SP positive anomalies can probably be due to (1) transient sources associated to shallow advection of fluids in the first meters of the ground (i.e. recent lava flows; Barde-Cabusson et al., 2009) and (2) deep convection in a hydrothermal system, affecting several hundred meters below the surface (wide-scale convection cells). A denser SP mapping could be compared to the map of the dated lava flows intersecting the rift zones in order to distinguish locally the sources of the SP signal among these two.

The SP signal variations between our 2006 and 2008 surveys highlight a strong increase of the signal (more than 350 mV) at the eastern limit of the main N–S rift zone and in the N120° rift zone and a significant decrease (up to –300 mV) on the N–S rift zone itself (Fig. 3d). At Piton de la Fournaise, structural analyses and geodetic measurements have shown that the central cone was affected by a preferential eastward motion (Letourneur et al., 2008; Peltier et al., 2009a and references therein). The flank instability can be explained by stress accumulation on the unbuttressed eastern flank due to the successive intrusions and accumulation of magma in the reservoir. The preferential motion of the eastern flank was especially well visible during the large distal eruption of April 2007 (Augier et al., 2008; Peltier et al., 2009b). Interferometric data reveal a motion of up to 80 cm of the eastern flank towards the sea (Augier et al., 2008). The dipolar SP signal observed: increase of the SP signal on the eastern limit of the N–S rift zone and decrease on the N–S rift zone itself can be due to an increase of the permeability along this eastern limit following the large eastward motion of the eastern flank during the April 2007 eruption. The SP decrease observed on the southern rift zone (maximum –300 mV) and on part of the northern rift zone (maximum –200 mV on DNW) can evidence an associated balancing of fluid flow circulation in the system. Hydrothermal fluids flow migrated to the more permeable area depleting the fluid supply in the main hydrothermal zones. Interestingly, no significant variation has been measured on the western part of the northern rift zone, on DS and DE. The fluid circulation inside these areas may be isolated from the rest of the system by their own fracture network, explaining why no disruption is observed.

## 5. Conclusions

The SP dataset collected in 2006 allowed us to build a global map of the Piton de la Fournaise's terminal cone and a detailed map of the summit area. We compared it to previous SP maps and confront our results to the geological history of the edifice to make the following conclusions, also synthesized on Fig. 7:

- (1) In addition to the strong SP anomalies characterizing the northern and southern rift zones, the N120° radial anomaly, and the

summit area, the entire terminal cone is affected by an extended hydrothermal activity, which prevents from observing a classical W-shaped SP signal of an active volcanic cone.

- (2) The main hydrothermal release has been identified inside the Dolomieu–Bory craters. Their limits are major structural barriers for fluid circulation.
- (3) The SP mapping in the Dolomieu crater reveals a hidden pre-existing east-dipping fracture or fault system, which controlled the Dolomieu collapse during the April 2007 eruptive crisis of Piton de la Fournaise.
- (4) As well, the former pit craters surrounding the Dolomieu–Bory craters appear as main fluid paths deeply connected to the central Dolomieu–Bory hydrothermal fluid path. Also the Petit Plateau SP anomaly having a larger extension than the visible associated fractures suggests that the pit crater has a greater extension at depth.
- (5) The SP increase between 2006 and 2008, along the eastern limit of the N–S rift zone, can be associated to the eastward motion of the eastern flank of the volcano during the April 2007 eruption.

SP anomalies can highlight zones of major permeability and of low mechanical resistance, and therefore of major probability of deformation, rupture and/or eruption. Using SP variations to distinguish eruption precursors and low mechanical resistance areas would require a continuous monitoring of the key areas showing the strongest SP anomalies.

## Acknowledgments

The field work was supported by The Université de la Réunion (BQR 2005–2006). We are particularly grateful to Benoît Fragnol and Frédéric Lorion for their help in acquiring the SP data in particularly wet and cold conditions. Logistic and field support from Laboratoire GéoSciences Réunion, Observatoire Volcanologique du Piton de la Fournaise, Benoît Welsch, Laurent Michon, Vincent Famin, Nicolas Villeneuve, and Alexandre Nercressian were greatly appreciated. We are grateful to Jean Vandemeulebrouck and Koki Aizawa whose comments helped to substantially improve the manuscript. This is IPGP contribution number 3197.

## References

- Aizawa, K., 2008. Classification of self-potential anomalies on volcanoes and possible interpretations for their subsurface structure. *Journal of Volcanology and Geothermal Research* 175 (3), 253–268. doi:10.1016/j.jvolgeores.2008.03.011.
- Aizawa, K., Uyeshima, M., Nogami, K., 2008. Zeta potential estimation of volcanic rocks on 11 island arc-type volcanoes in Japan: implication for the generation of local self-potential anomalies. *Journal of Geophysical Research* 113, B02201. doi:10.1029/2007JB005058.
- Aizawa, K., Ogawa, Y., Ishido, T., 2009. Groundwater flow and hydrothermal systems within volcanic edifices: delineation by electric self-potential and magnetotellurics. *Journal of Geophysical Research*, B: Solid Earth 114.
- Aizawa, K., Kanda, W., Ogawa, Y., Iguchi, M., Yokoo, A., Yakiwara, H., Sugano, T., 2011. Temporal changes in electrical resistivity at Sakurajima volcano from continuous magnetotelluric observations. *Journal of Volcanology and Geothermal Research* 199 (1–2), 165–175. doi:10.1016/j.jvolgeores.2010.11.003.
- Augier, A., Froger, J.L., Cayol, V., Fukushima, Y., Tinar, P., Souriot, T., Mora, O., Staudacher, T., Durand, P., Fruneau, B., Villeneuve, N., 2008. The April 2007 eruption at Piton de la Fournaise, Réunion Island, imaged with ENVISAT-ASAR and ALOS-PALSAR data. *USEReST Workshop*, Napoli, Italy.
- Bachèlery, P., 1981. Le Piton de la Fournaise (Ile de la Réunion). Etude volcanologique, structurale et pétrologique. PhD thesis, Univ. Clermont-Ferrand II, 215 pp.
- Barde-Cabusson, S., Levieux, G., Lénat, J.-F., Finizola, A., Revil, A., Chaput, M., Dumont, S., Duputel, Z., Guy, A., Mathieu, L., Saumet, S., Sorbadère, F., Vieille, M., 2009. Transient self-potential anomalies associated with recent lava flows at Piton de la Fournaise Volcano (Réunion Island, Indian Ocean). *Journal of Volcanology and Geothermal Research* 187, 158–166. doi:10.1016/j.jvolgeores.2009.09.003.
- Bedrosian, P.A., Unsworth, M.J., Johnston, M.J.S., 2007. Hydrothermal circulation at Mount St. Helens determined by self-potential measurements. *Journal of Volcanology and Geothermal Research* 160, 137–146.
- Boubekraoui, S., Aubert, M., 1999. Apport de la méthode des potentiels spontanés à la reconnaissance géologique et hydrogéologique des terrains volcaniques superficiels du Grand-Brûlé (Réunion, Océan Indien). *Hydrogéologie* 1, 43–51.
- Carter, A., van Wyk de Vries, B., Kelfoun, K., Bachèlery, P., Briole, P., 2007. Pits, rifts and slumps: the summit structure of Piton de la Fournaise. *Bulletin of Volcanology* 69, 741–756. doi:10.1007/s00445-006-0103-4.



- Corwin, R.F., 1997. The self-potential method for environmental and engineering applications: geotechnical and environmental geophysics. In: Ward, H. (Ed.), *Investigations in Geophysics: Soc. Expl. Geophys.*, vol. 5, p. 1.
- Finizola, A., Lénat, J.-F., Macedo, O., Ramos, D., Thouret, J.-C., Sortino, F., 2004. Fluid circulation and structural discontinuities inside Misti volcano (Peru) inferred from self-potential measurements. *Journal of Volcanology and Geothermal Research* 135, 343–360.
- Finizola, A., Revil, A., Rizzo, E., Piscitelli, S., Ricci, T., Morin, J., Angeletti, B., Mocochain, L., Sortino, F., 2006. Hydrogeological insights at Stromboli volcano (Italy) from geoelectrical, temperature, and CO<sub>2</sub> soil degassing investigations. *Geophysical Research Letters* 33, L17304. doi:10.1029/2006GL026842.
- Finizola, A., Aubert, M., Revil, A., Schütze, C., Sortino, F., 2009. Importance of structural history in the summit area of Stromboli during the 2002–2003 eruptive crisis inferred from temperature, soil CO<sub>2</sub>, self-potential, and electrical resistivity tomography. *Journal of Volcanology and Geothermal Research* 183, 213–227. doi:10.1016/j.jvolgeores.2009.04.002.
- Finizola, A., Ricci, T., Deiana, R., Barde-Cabusson, S., Rossi, M., Praticelli, N., Giocoli, A., Romano, G., Delcher, E., Suski, B., Revil, A., Menny, P., Di Gangi, F., Letort, J., Peltier, A., Villasante-Marcos, V., Douillet, G., Avard, G., Lelli, M., 2010. Adventive hydrothermal circulation on Stromboli volcano (Aeolian Islands, Italy) revealed by geophysical and geochemical approaches: implications for general fluid flow models on volcanoes. *Journal of Volcanology and Geothermal Research* 196, 111–119. doi:10.1016/j.jvolgeores.2010.07.022.
- García, X., Jones, A.G., 2010. Internal structure of the western flank of the Cumbre Vieja volcano, La Palma, Canary Islands, from land magnetotelluric imaging. *Journal of Geophysical Research, B: Solid Earth* 115 (12), B07104. doi:10.1029/2009jb006445.
- Guichet, X., Zuddas, P., 2003. Effect of secondary minerals on electrokinetic phenomena during water–rock interaction. *Geophysical Research Letters* 30 (13), 1714. doi:10.1029/2003GL017480.
- Hase, H., Ishido, T., Takakura, S., Hashimoto, T., Sato, K., Tanaka, Y., 2003.  $\zeta$  potential measurement of volcanic rocks from Aso caldera. *Geophysical Research Letters* 30 (23), 2210. doi:10.1029/2003GL018694.
- Ishido, T., 2004. Electrokinetic mechanism for the “W”-shaped self-potential profile on volcanoes. *Geophysical Research Letters* 31, L15616. doi:10.1029/2004GL020409.
- Ishido, T., Kiruchi, T., Matsushima, N., Yano, Y., Nakao, S., Sugihara, M., Toshi, T., Takakura, S., Ogawa, Y., 1997. Repeated self potential profiling of Izu-Oshima Volcano, Japan. *Journal of Geomagnetism and Geoelectricity* 49, 1267–1278.
- Join, J.-L., Folio, J.-L., Robineau, B., 2005. Aquifers and groundwater within active shield volcanoes. Evolution of conceptual models in the Piton de la Fournaise volcano. *Journal of Volcanology and Geothermal Research* 147, 187–201. doi:10.1016/j.jvolgeores.2005.03.013.
- Lénat, J.-F., 1987. Structure et Dynamique internes d’un volcan basaltique intraplaque océanique: Le Piton de la Fournaise (Ile de la Réunion). PhD thesis, Université Blaise Pascal, Clermont-Ferrand, France.
- Lénat, J.-F., 2007. Retrieving self-potential anomalies in a complex volcanic environment: an SP/elevation gradient approach. *Near Surface Geophysics* 5, 161–170.
- Lénat, J.-F., Bachèlery, P., 1990. Structure et fonctionnement de la zone centrale du Piton de la Fournaise. In: Dans, Lénat, J.-F. (Eds.), *Le volcanisme de la Réunion – Monographie. Cent. Rech. Volcanol.*, Clermont-Ferrand, France, pp. 257–296.
- Lénat, J.F., Fitterman, D., Jackson, D.B., Labazuy, P., 2000. Geoelectrical structure of the central zone of Piton de la Fournaise volcano (Réunion). *Bulletin Volcanologique* 62, 75–89.
- Letourneur, L., Peltier, A., Staudacher, T., Gudmundsson, A., 2008. The effects of rock heterogeneities on dyke paths and asymmetric ground deformation: The example of Piton de la Fournaise (Réunion Island). *Journal of Volcanology and Geothermal Research* 173 (3–4), 289–302.
- Levieux, G., 2004. Construction d’une carte régionale de polarisation spontanée au Piton de la Fournaise. Université Blaise Pascal, Clermont-Ferrand, France, Analyse des anomalies. Mémoire de Travail d’Étude et de Recherche de Maîtrise Thesis. 64 pp.
- Linde, N., Jougnot, D., Revil, A., Matthai, S.K., Arora, T., Renard, D., Doussan, C., 2007. Streaming current generation in two-phase flow conditions. *Geophysical Research Letters* 34 (3), L03306. doi:10.1029/2006GL028878.
- Malengreau, B., Lénat, J.-F., Bonneville, A., 1994. Cartographie et surveillance temporelle des anomalies de Polarisation Spontanée (PS) sur le Piton de la Fournaise. *Bulletin de la Société Géologique de France* 165, 221–232.
- Massenet, F., Pham, V.N., 1985. Experimental and theoretical basis of self-potential phenomena in volcanic areas with reference to results obtained on Mount Etna (Sicily). *Earth and Planetary Science Letters* 73, 415–429.
- Michel, S., Zlotnicki, J., 1998. Self-potential and magnetic surveying of la Fournaise volcano (Réunion Island): correlations with faulting, fluid circulation and eruption. *Journal of Geophysical Research* 103 (NO B8), 17,845–17,857.
- Michon, L., Staudacher, Th., Ferrazzini, V., Bachèlery, P., Marti, J., 2007a. April 2007 collapse of Piton de la Fournaise: a new example of caldera formation. *Geophysical Research Letters* 34, L21301. doi:10.1029/2007GL031248.
- Michon, L., Saint-Ange, F., Bachèlery, P., Villeneuve, N., Staudacher, Th., 2007b. Role of the structural inheritance of the oceanic lithosphere in the magmato-tectonic evolution of Piton de la Fournaise volcano (La Réunion Island). *Journal of Geophysics* 112, B04205. doi:10.1029/2006JB004598.
- Michon, L., Cayol, V., Letourneur, L., Peltier, A., Villeneuve, N., Staudacher, T., 2009a. Edifice growth, deformation and rift zone development in basaltic setting: insights from Piton de la Fournaise shield volcano (Reunion Island). *Journal of Volcanology and Geothermal Research* 184 (1–2), 14–30. doi:10.1016/j.jvolgeores.2008.11.002.
- Michon, L., Villeneuve, N., Catry, Th., Merle, O., 2009b. How summit calderas collapse on basaltic volcanoes: new insights from the April 2007 caldera collapse of Piton de la Fournaise volcano. *Journal of Volcanology and Geothermal Research* 184 (1–2), 138–151. doi:10.1016/j.jvolgeores.2008.11.003.
- Nourbehecht, B., 1963. Irreversible thermodynamic effects in inhomogeneous media and their applications in certain geoelectric problems. Ph.D. Thesis, Mass. Inst. Of Technology, Cambridge.
- Overbeek, J.T.G., 1952. Electrochemistry of the double layer. In: Kruyt, H.R. (Ed.), *Colloid Science: Irreversible Systems*, vol. 1. Elsevier Sci, New York, pp. 115–193.
- Peltier, A., Bachèlery, P., Staudacher, T., 2009a. Magma transport and storage at Piton de la Fournaise (La Réunion Island) between 1972 and 2007: a review of geophysical and geochemical data. *Journal of Volcanology and Geothermal Research* 184 (1–2), 93–108.
- Peltier, A., Staudacher, T., Bachèlery, P., Cayol, V., 2009b. Formation of the April 2007 caldera collapse at Piton de la Fournaise volcano: insights from GPS data. *J. Volcano. Geotherm. Res.* 184 (1–2), 152–163.
- Revil, A., 2002. Comment on “Rapid fluid disruption: a source for self-potential anomalies on volcanoes” by M. J. S. Johnston, J. D. Byerlee, and D. Lockner. *Journal of Geophysical Research* 107 (B8). doi:10.1029/2001JB000788.
- Revil, A., Cerepi, A., 2004. Streaming potential in two-phase flow condition. *Geophysical Research Letters* 31 (11), L11605. doi:10.1029/2004GL020140.
- Revil, A., Saracco, G., Labazuy, P., 2003. The volcano-electric effect. *Journal of Geophysical Research* 108, B5. doi:10.1029/2002JB001835.
- Revil, A., Johnson, T.C., Finizola, A., 2010. Three-dimensional resistivity tomography of Vulcan’s forge, Vulcano Island, southern Italy. *Geophysical Research Letters* 37, L15308. doi:10.1029/2010gl043983.
- Revil, A., Finizola, A., Sortino, F., Ripepe, M., 2004. Geophysical investigations at Stromboli volcano, Italy. Implications for ground water flow and paroxysmal activity. *Geophysical Journal International* 157, 426–440. doi:10.1111/j.1365-246X.2004.02181.x.
- Revil, A., Finizola, A., Piscitelli, S., Rizzo, E., Ricci, T., Crespy, A., Angeletti, B., Balasco, M., Barde Cabusson, S., Bennati, L., Bolève, A., Byrdina, S., Carzaniga, N., Di Gangi, F., Morin, J., Perrone, A., Rossi, M., Roulleau, E., Suski, B., 2008. Inner structure of La Fossa di Vulcano (Vulcano Island, southern Tyrrhenian Sea, Italy) revealed by high resolution electric resistivity tomography coupled with self-potential, temperature, and CO<sub>2</sub> diffuse degassing measurements. *Journal of Geophysical Research* 113, B07207. doi:10.1029/2007JB005394.
- Revil, A., Finizola, A., Ricci, T., Delcher, E., Peltier, A., Barde-Cabusson, S., Avard, G., Bailly, T., Bennati, L., Byrdina, S., Colonge, J., Di Gangi, F., Douillet, G., Lupi, M., Letort, J., Tsang Hin Sun, E., 2011. Hydrogeology of Stromboli volcano, Aeolian Islands (Italy) from the interpretation of resistivity tomograms, self-potential, soil temperature, and soil CO<sub>2</sub> concentration measurements. *Geophysical Journal International* 186, 1078–1094. doi:10.1111/j.1365-246X.2011.05112.x.
- Sill, W.R., 1983. Self potential modeling from primary flows. *Geophysics* 48, 76–86.
- Staudacher, T., 2010. Field observations of the 2008 summit eruption at Piton de la Fournaise (Ile de la Réunion) and implications for the 2007 Dolomieu collapse. *Journal of Volcanology and Geothermal Research* 191, 60–68.
- Urai, M., Geshi, N., Staudacher, T., 2007. Size and volume evaluation of the caldera collapse on Piton de la Fournaise volcano during the April 2007 eruption using ASTER stereo imagery. *Geophysical Research Letters* L22318. doi:10.1029/2007GL031551.
- Yasukawa, K., Ishido, T., Suzuki, I., 2005. Geothermal reservoir monitoring by continuous self-potential measurements, Mori geothermal field, Japan. *Geothermics* 34 (5), 551–567. doi:10.1016/j.geothermics.2005.04.005.
- Zlotnicki, J., Michel, S., Annen, C., 1994. Anomalies de polarisation spontanée et systèmes convectifs sur le volcan du Piton de la Fournaise (Ile de Réunion, France). *Comptes Rendus de l’Académie des Sciences Serie Ila:Sciences de la Terre et des Planètes* 318, 1325–1331.
- Zlotnicki, J., Boudon, G., Viode, J.P., Delarue, J.F., Mille, A., Bruere, F., 1998. Hydrothermal circulation beneath Mount Pelee inferred by self potential surveying. Structural and tectonic implications. *Journal of Volcanology and Geothermal Research* 84, 73–91.